Received: 22 January 2021 | Revised: 21 April 2021 | Accepted: 12 May 2021

DOI: 10.1111/ijag.16144

INTERNATIONAL JOURNAL OF Applied Glass SCIENCE

SPECIAL ISSUE ARTICLE

Low-alkali borosilicate glass microspheres from waste cullet prepared by flame synthesis

Pavel Larionau[1] | **Miroslava Hujova**[2] | **Monika Michalková**[3] | **Mokhtar Mahmoud**[2] | **Anna Švančárková**[2] | **Dagmar Galusková**[2] | **Milan Parchoviansky**[2] | **Enrico Bernardo**[4] | **Dušan Galusek**[2,3] | **Jozef Kraxner**[2]

[1]Glass and Ceramic Technology Department, Belarusian State Technological University, Minsk, Belarus

[2]FunGlass, Alexander Dubcek University of Trencin, Trencin, Slovakia

[3]Joint Glass Centre of the IIC SAS, TnUAD, and FChFT STU, Trencin, Slovakia

[4]Dipartmento di Ingegneria Industriale Università degli Studi di Padova, Padova, Italy

Correspondence
Miroslava Hujova, FunGlass, Alexander Dubcek University of Trencin, Trencin, Slovakia.
Email: miroslava.hujova@tnuni.sk

Funding information
Vedecká Grantová Agentúra MŠVVaŠ SR a SAV, Grant/Award Number: 1/0456/20 and 2/0091/20; Horizon 2020 Framework Programme, Grant/Award Number: 739566

Abstract

Although glass recycling is considered to be a default method for glass waste management, fine fractions of container soda-lime glass, or cullet of other compositions are still landfilled. This happens despite existing alternatives. Success could lie in advanced upcycled products that bring higher economic motivation for the implementation in industry, but these are often connected to alternative ways of product synthesis. We provide an example of waste glass upcycling by the preparation of glass microspheres (GM) from specialty low-sodium alumino borosilicate-based glasses via flame synthesis (FS). GM and the precursors, either from colorless medical vials or glass fibers, were characterized by scanning electron microscopy (SEM), simultaneous thermal analysis coupled with differential thermal analysis (STA-DTA), and image analysis. A dynamic corrosion test was performed and evaluated via ion-coupled plasma with optical emission spectroscopy (ICP-OES) to observe corrosion kinetics products. FS has proved to be a fast method of waste glass processing into GM. This article, besides the characterization of the starting material and final products, also suggests the possibility of processing for other landfilled waste glasses and also discusses the manufacturing of GM for water filters and fillers for polymers.

KEYWORDS

waste upcycling, flame synthesis process, glass microspheres, materials characterization, hydrolytic stability

1 | INTRODUCTION

The growing amounts of glass waste are ascribed to the growing consumption of products and strict emphasis on high-quality production. Taking into account that 76% of glass waste is recycled in the EU[1] and 33% in North America,[2] each year, thousand tonnes of glass are landfilled. Even in the case of the most recycled soda-lime container glass, fine fractions (<30 μm) are still landfilled, due to the plastic and metal contaminations.[3,4]

During the glass waste treatment, the unrecyclable cullet is sorted out in energetically and technologically expensive procedures,[5] only for then being landfilled. This happens with medical glasses,[6] lead/barium crystal glasses, and also glass

fibers and their composites.[7] These glasses are also oftentimes landfilled directly from their manufacture, if products are faulty. Their reintroduction in a glass batch would cause too many serious technological problems, that is, stones or streaks.[8,9]

Out of the mentioned examples, medical glasses and glass fibers are of the most significant value. These glasses are of a low-alkali alumino-borosilicate formulation, well-known since the beginning of the 20th century.[10] They are characteristic in their hydrolytic resistance,[11] low thermal expansion coefficient,[12] high electrical resistivity,[13] and low dielectric constant.[14]

In lieu of recycling, upcycling could be the answer to cullet landfilling. The aim of upcycling is to provide a product, different from the original one, but possessing an added economic value. Upcycling options for borosilicate glasses include the conversion of cullet into glass foams [7,15-19] or geopolymers.[20-23] However, the practical implementations are limited because of (a) the necessity to transport the waste from several distant producing facilities into a processing facility, (b) mixed material characterization, and (c) the material processed on the industrial scale needs to be produced in large and steady quantities.[20] Also, traditional construction materials are oftentimes protected by strict legislation.[24] These issues could be partially avoided if the upcycling focused on highly specialized products.

To upcycle the borosilicate cullet into an economically advantageous product, we suggest the production of glass microspheres (GM) via flame synthesis (FS) technology. According to a research report, the global GM market reached 1993.36 million USD by 2019, growing annually by 12.4%.[26,27] GM can be produced as solid/full (FGM), hollow (HGM), and porous (PGM).[25-29] The manufacturing process starts with the feeding of a precursor into a high-temperature flame (~2200°C), where particles almost immediately melt. Molten glass particles are hyperquenched in a spray of deionized water and the structure solidifies in the form of GM of particular morphology (FGM, HGM, PGM). These unique conditions can also lead to a wide spectrum of glasses usually characterized by high melting temperatures and rapid crystallization.[33,34]

The resulting GM of various types shows excellent heat resistance, light weight, porosity, and mechanical properties. These properties make them advantageous in aviation and the automotive industry,[34] and construction.[35-37] GM are also considered for hydrogen storage,[30,38-41] energy-saving applications (thermal insulation), and also as luminescent or reflective materials.[42-44] Recently GM have proven to be versatile biomaterials.[45-47]

GM are favorable for the manufacture of complex-shaped glass articles by additive manufacturing (AM) technologies. The replacement of glass frit by GM leads to lower friction during feeding, and increased packing density of product.[48] AM technologies produce macroporous green structures, which upon sintering might be complemented by a microporosity. The possibility to produce hierarchical porosity from hydrolytically stable waste cullet would be interesting for the design of water filters.[49] Yet, the chemical safety of the product would still have to be assessed via hydrolytic durability tests, due to the possible composition changes caused by FS.

The final argument for upcycling by the FS, versus recycling, lies in the energetic aspect of the process. The embodied energy for the production of glass articles, which is the amount of energy used in the primary production, is in the orders of 10 MJ/kg. Yet the saving in embodied energy during cullet recycling is not more than 25%.[50] This is due to the energetically demanding cullet sorting step,[5,51,52] hence the energy savings are not sufficiently motivating when considering the technological complexity of recycling.

This publication aims to demonstrate the synthesis of GM solely from low-alkali borosilicate glass waste. Input materials and final products were characterized in the terms of their physical and chemical properties. We were able to produce hydrolytically stable FGM from the medical glass. A promising synthesis of PGM from glass fibers indicates a future successful production after synthesis adjustments.

2 | EXPERIMENTAL PROCEDURE

The raw materials were received directly from their manufacturers: Glass fibers (GF) from Johns Manville Slovakia, and colorless medical vials (MV) from MediGlass Slovakia (Nouva Ompi Group). The chemical compositions of input materials, provided in Table 1, were measured by the Bruker Tiger S8 X-ray fluorescence spectrometer (WDXRF).

GF and MV were crushed in an agate mortar and sieved to obtain a sufficient amount of glass powder (precursor) with a mean particle size of 40–80 μm. This powder served as both the precursor for FS and a testing sample for the stated analyses. A general scheme of the in-house built FS apparatus is provided in Figure 1.[31]

For FS the O_2/CH_4 mixture was used that yielded a flame with the temperature of ~2200°C. The FS laboratory device is based at the FunGlass Centre (Trencin, Slovakia) and was approved as a utility model[31] with the overall efficiency of the device in the range of 75%–85%. The production rate of GM was 2 g/min using oxygen carrier gas (0.016 m^3/min) and oxygen - methane flame at the consumption of gasses, O_2–0.042 m^3/min and CH_4 - 0.078 m^3/min. The prepared precursors from GF and MV were fed into a torch with a vacuum powder feeder at the rate of 3.3 (GF) and 4.8 (MV) g min^{-1}. The molten particles were quenched in the spray of deionized water and then micro-filtered through a ceramic filter (porosity <0.3 μm). Products were dried overnight at ~120°C. The total yield was 54% for GF-GM and 63% for MV-FGM.

TABLE 1 The composition of waste glasses (precursors for the flame synthesis) measured by WDXRF in wt%, standard deviations are estimated from three consequential measurements

	Glass fibers (GF)		Medical vials (MV)	
	Composition (wt%)	Standard deviation	Composition (wt%)	Standard deviation
SiO_2	55.20	0.700	71.70	0.700
Al_2O_3	14.30	0.200	6.68	0.050
Fe_2O_3	0.31	0.003	<0.10	<0.001
TiO_2	0.37	0.004	0.02	0.001
CaO	22.80	0.200	1.05	0.030
BaO	0.04	0.002	0.74	0.030
MgO	0.63	0.010	—	—
Na_2O	0.37	0.010	6.53	0.090
K_2O	0.72	0.008	1.32	0.030
B_2O_3	4.40	0.300	9.80	0.400
SO_3	0.01	0.001	0.01	0.400

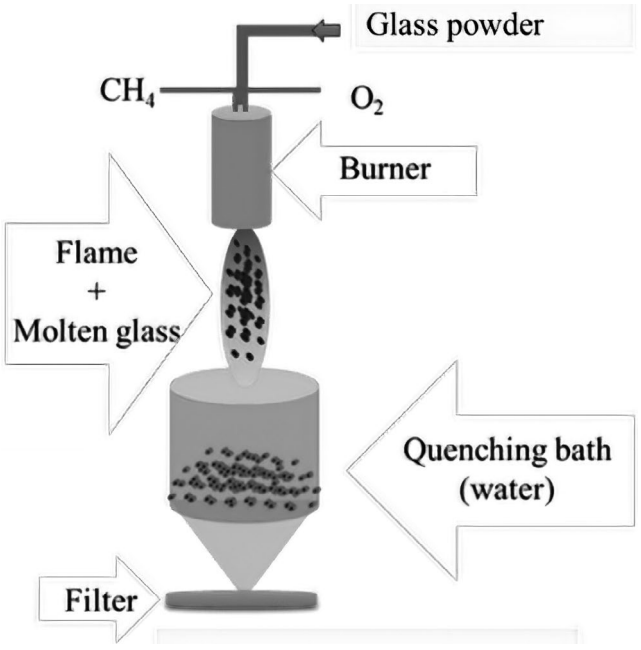

FIGURE 1 Scheme of the flame synthesis apparatus in the laboratory scale. Glass powder is fed into the feeding gasses, and due to high temperatures, it is instantly molten. Droplets are hyperquenched in the stream of coolant and collected on the filter

To address the mineralogy of products, powder X-ray diffraction was used (XRD; Panalytical Empyrean DY1098 B.V. Netherlands) Cu$K\alpha$ radiation, 2θ range 10°–80°. Afterward, the surface and the cross sections of the GM were examined by scanning electron microscope (SEM; Jeol JSM 7600 F), 15 kV acceleration voltage, 14 mm work distance (WD) using lower secondary electron detector (LEI). Approximate compositions were obtained through the electron dispersion spectroscopy (EDS), 5 kV acceleration voltage, 11 mA, 14 mm WD. For cross-sectional examination, the samples were mounted into Trans Optic resin (Buehler) and were polished using Buehler Planar Met 300. The SEM micrographs were also used to evaluate the GM size and size distribution, using the Image analysis performed in NIS Elements Viewer. The density of the obtained glass microspheres was measured by liquid pycnometry in isopropanol.[53]

Characteristic thermal properties of GM, the glass-transition temperature (T_g), and the maximum of the first crystallization peak temperature (T_c) were determined using simultaneous thermal analysis coupled with differential thermal analysis (STA-DTA; Netzsch STA 449 F1 Jupiter Netzsch GmbH& Co., Bad Berneck Germany). The heating rate used was 10 K min^{-1}, at the N_2 of 25 mL min^{-1} used as the carrier gas. The values were obtained on the first DTA curve, the values of T_g were evaluated on the onset of the first derivation glass-transition peak.

The chemical resistance tests were performed in dynamic test mode. Samples (0.5 g) were measured in corrosion cells, with one cell left empty for the blank test line. Deionized water (DIW) at ~90°C was chosen as the testing solvent, at the steady flow rate ~30 mL h^{-1}, the test duration was 8 h total. Leachates were collected after every 30 min during the first 2 h. Afterward, the sampling was performed every hour.

Leachates were immediately stabilized by the addition of 1 ml 1 M HNO_3 solution and analyzed by optical emission spectroscopy in inductively coupled plasma (ICP-OES; Agilent 5100). The measurements were carried out with the scandium (10 mg L^{-1}) as the internal standard to deal with non-spectral interferences.

3 | RESULTS AND DISCUSSION

The mineralogical analysis of GF-GM and MV-GM, shown in Figure 2, confirmed the microspheres were XRD

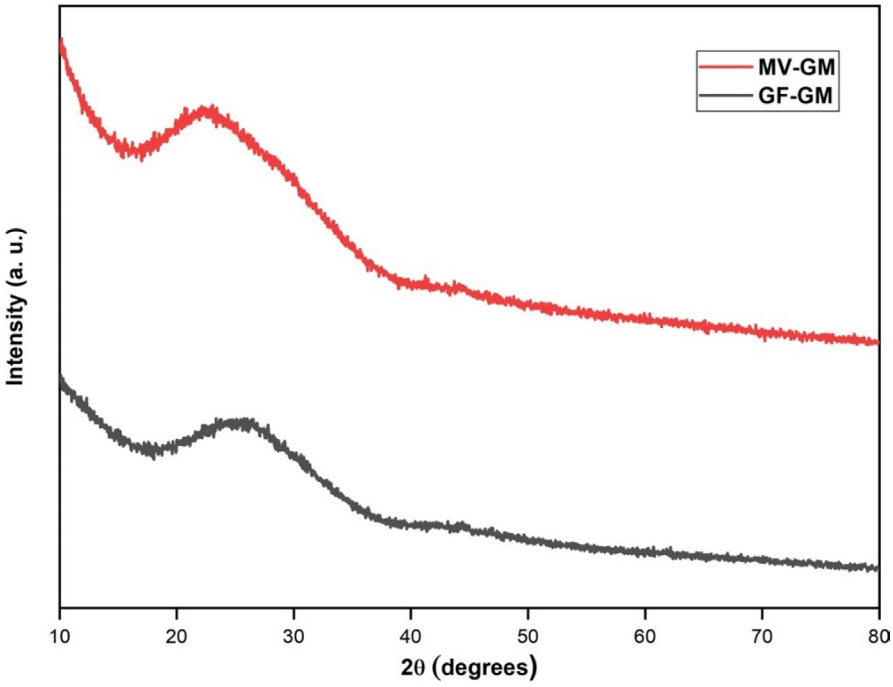

FIGURE 2 XRD patterns of GF-GM and MV-GM proving the GM upon FS were XRD amorphous

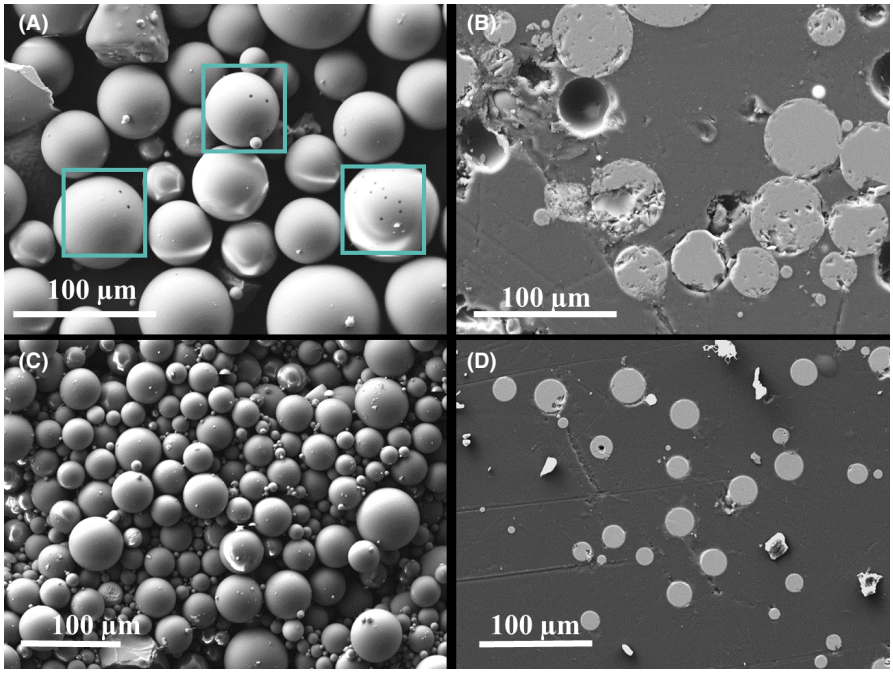

FIGURE 3 GF-GM (A) surface view (residual pores captured in brackets), (B) cross section; and MV-FGM (C) surface view, (D) cross section

amorphous, with the characteristic halo of silicate vitreous phase at $2\theta = 20°–35°$. We conclude that processing low-alkali borosilicate waste glasses by FS yields materials that are not prone to crystallization, and hence the process is in this aspect without major technological difficulties.

SEM results for GF-GM are shown in Figure 3A in the surface viewing and Figure 3B in cross section. Some residual pores in the microspheres, for better visualization highlighted in the brackets, indicate that the resin coating of GF precursors decomposed during FS. However, only small amounts of closed pores are visible, and only in larger GM specimens. Yet, this claim is also confirmed by the pycnometer tests. The density of GF-GM (2.5 ± 0.2 g/cm^3) showed a small deviation from the starting glass residue (2.6 ± 0.1 g/cm^3).

Figure 3C,D show that FS yielded full MV-GM, without any pores visible on the surface or in the cross section. The achievement of full density was confirmed by the fact that the density of MV-GM (2.4 ± 0.2 g/cm^3) exactly matched that of the starting cullet (2.4 ± 0.2 g/cm^3).

Table 2 provides the average compositions obtained by SEM-EDS on the surface and the cross section of the

TABLE 2 Composition of glass microspheres obtained via SEM-EDX in wt%. and compared to the values from precursors measured by XRF. Arrows show the apparent concentration change in the GM against the precursor of corresponding compositions

	GF		MV	
	Precursor	**GM**	**Precursor**	**GM**
SiO_2	55.2	56.0	71.7	79.0
B_2O_3	4.4	4.6	9.8	9.0
Na_2O	0.4	0.1	6.5	4.5
Al_2O_3	14.3	14.0	6.7	6.0
K_2O	0.7	—	1.3	—
CaO	22.8	24.0	1.1	1.7
TiO_2	0.4	0.4	—	—
MgO	0.6	0.6	—	—
Fe_2O_3	0.3	—	—	—

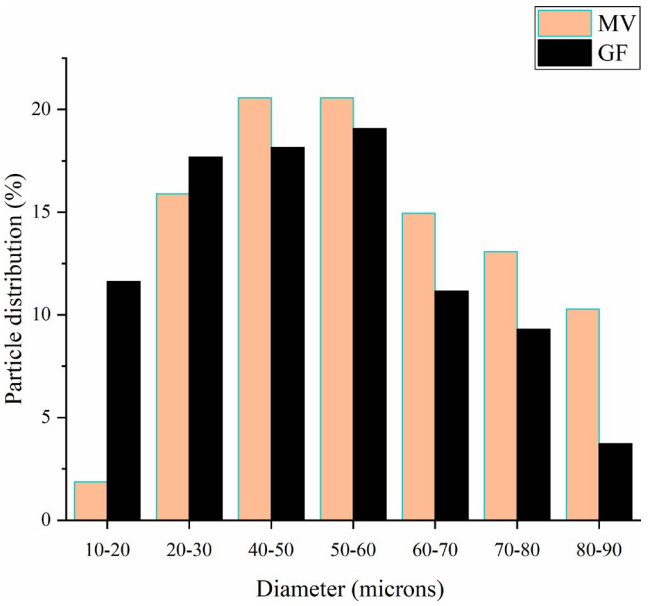

FIGURE 4 Particle size distribution in respect to group sizes of particles. GF-GM show a significant population of particles under the sieving limit

respective GM. When comparing with the results obtained by XRF (Table 1), some changes in the measured values were observed, with possible volatilization of alkalis and B_2O_3. It is reasonable to conclude that the FS and consequential quenching did not alter the chemical composition of GM significantly, despite the different analytical methods used. The chemical composition of the product remains characteristic for low-alkali alumino-borosilicate glasses. The properties bound to the chemical composition of the original waste can be assumed also for the upcycled product.

Images obtained from the SEM analysis were evaluated to determine the mean GM diameter and size distribution, also shown in Figure 3 as the distribution of particle size. In the case of GF-GM, ~50% of particles were 40–60 μm in diameter, with a significant ratio of GM under the mean value. This could be explained by the diameter of each fiber from the GF bundle being considerably smaller than the mean size of the sieve used for this purpose. MV-FGM were also mostly yielded in the mean fraction of 40–60 μm, ~50% total, but considering the fact the precursor originates from bulky material, the particle sizes remained evenly distributed across the entire size range (10–80 μm). In both cases, particles above the sieving limit were detected, which could result from either large particle aspect ratios, too high FS temperature resulting in the sintering of small particles, or bloating of particles due to entrapped pores (Figure 4).

The DTA results are shown in Figure 5 and consequentially summarized in Table 3. In both cases, GM demonstrated higher values of T_g and T_c than those of their precursors. This shift cannot be ascribed entirely to the changes in the thermal history of GM, because the composition of GM has also changed slightly (Table 2). The presented microspheres show a wide temperature interval between T_g and T_c, comparable to that of the precursors. This parameter is important, if GM should be considered for the manufacture of water filters by AM technologies. In this case, hierarchical porosity is achieved first by printing and then by sintering. A sufficiently broad temperature interval where viscous flow sintering can be applied (sintering window) is, therefore, an important parameter in the process.

Figure 6 shows the dissolution rate of GM expressed in terms of the cumulative concentration rates of Si and Al, which represent the glass-forming elements. MV-GM dissolved at a much slower rate compared to that of GF-GM, reaching the state very near to solubility plateau.[55] The product maintained excellent hydrolytic resistance, which is an important property in applications involving higher humidity (air filters) or aqueous solutions (cleaning of wastewater). Porosity could be introduced into MV-GM by chemical means, for example, by alkali activation.[56] The introduction of the pores into GM would broaden the hierarchical porosity in future water filters.

The measured amounts of Si and Al leached from GF-GM were higher. Considering the lower content of silica in the GF, we can conclude that the GF-GM dissolve faster than the GM prepared from medical glass. This is in line with the known high hydrolytic resistance of borosilicate medical glass. The prepared GF-GM also showed a small number of pores (Figure 3) without any preconditioning of precursor. Their porosity could be enhanced by chemical pretreatments, which would result in a porous lightweight material. The GF-GM could be then suitable also for other applications than water filtration, such as lightweight fillers in polymers.

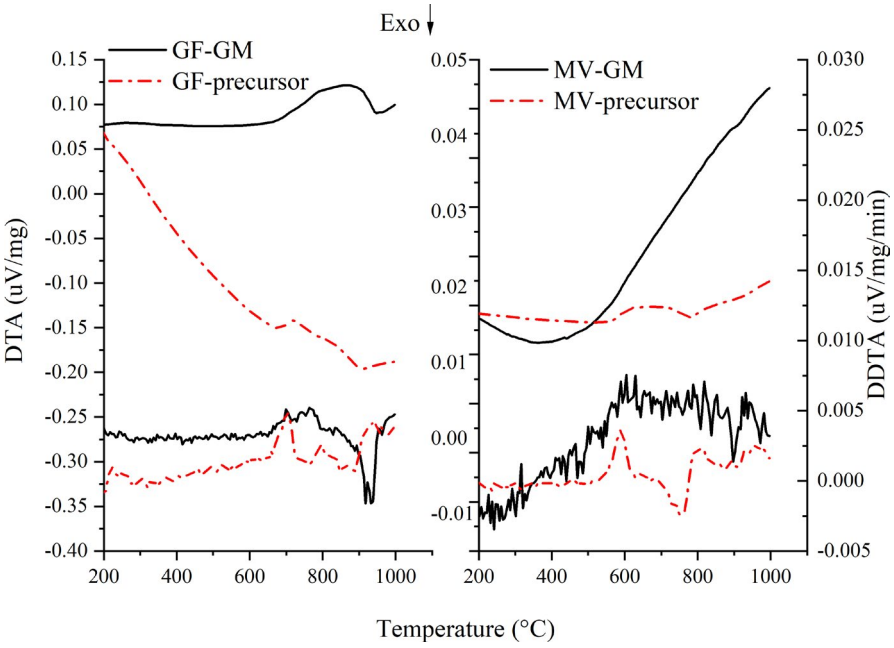

FIGURE 5 DTA curves for GF precursor and GM (left) and MV precursor and GM (right). The T_g and T_c temperatures were estimated by the first derivation of the curve

TABLE 3 T_g and T_c (in °C) for precursors and products of FS

	T_g (°C)	T_c (°C)
GF	703	877
GF-GM	750	948
MV	585	790
MV–GM	605	920

4 | CONCLUSION

Landfilled glass waste represents an unnecessary ecological burden and wasted economical potential. In this study, we have proven that low-alkali borosilicate glasses, namely glass fibers, and medical vials, are an excellent material for the preparation of glass microspheres, a material of large potential for utilization and functionalization. The results show that through flame synthesis, we can produce either solid or porous glass microspheres. In the latter case, we observed only a small number of pores. However, the used precursor was without any prior adjustments and the preconditioning and/or changes in the synthesis conditions could lead to a more porous product in the future.

The resulting products are characteristic by a wide sintering window, and good particle size-control, both of which offer opportunities for further functionalization. In the case of microspheres prepared from medical vials, excellent hydrolytic resistance was preserved, despite the large active surface. The microspheres are considered excellent raw materials for the preparation of water filters by AM technologies. The microspheres from glass fibers dissolved at comparably faster rates. We, therefore, recommend their use in environments where they are not in direct contact with humidity/aqueous solutions.

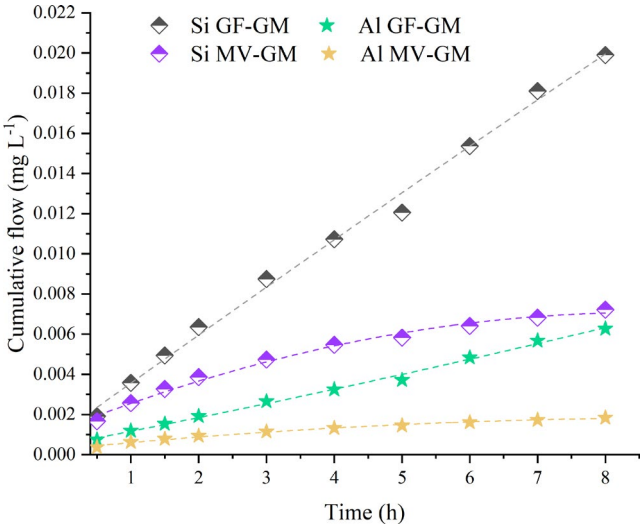

FIGURE 6 The cumulative flow for GF and MV GM was expressed in the terms of glass-forming element concentrations (Si and Al), during the first 8 h of dynamic corrosion testing

ACKNOWLEDGMENTS

This paper is a part of the dissemination activities of project FunGlass. This project has received funding from the European Union´s Horizon 2020 research and innovation program under grant agreement No 739566. The authors also gratefully acknowledge the financial support from the Slovak Grant Agency of Ministry of Education, Science, Research and Sport, VEGA Nr 2/0091/20 and 1/0456/20 Mr Larionau's training was possible due to the support of Slovak academic information agency SAIA.

ORCID

Miroslava Hujova https://orcid.org/0000-0003-0876-7292
Milan Parchoviansky https://orcid.org/0000-0002-1267-9220
Enrico Bernardo https://orcid.org/0000-0003-4934-4405
Dušan Galusek https://orcid.org/0000-0001-5995-8780

REFERENCES

1. FEVE. Record Collection of Glass Containers for Recycling hits 76% in the EU [Internet]. The European Container Glass Federation. Brussels; 2019. Available from: https://FEVE.org/about-glass/statistics/
2. Jacoby M. Why glass recycling in the US is broken. Chem News. 2019;97(6).
3. Monich PR, Dogrul F, Lucas H, Friedrich B. Strong porous glass-ceramics from alkali-activation and sinter-crystallization of vitrified MSWI bottom ash. 2019;08:101–8.
4. Sorting and contaminant removal for recycling glass [Internet]. Available from: https://www.sesotec.com/emea/en/industries/sub/glass
5. Bonifazi G, Serranti S. Imaging spectroscopy based strategies for ceramic glass contaminants removal in glass recycling. Waste Manag [Internet]. 2006;26(6):627–39. Available from http://www.sciencedirect.com/science/article/pii/S0956053X05001649.
6. Rincon Romero A, Marangoni M, Cetin S, Bernardo E. Recycling of inorganic waste in monolithic and cellular glass-based materials for structural and functional applications. J Chem Technol Biotechnol. 2016;91(7):1946–61.
7. Ramteke DD, Hujova M, Kraxner J, Galusek D, Romero AR, Falcone R, et al. Up-cycling of 'unrecyclable' glasses in glass-based foams by weak alkali-activation, gel casting and low-temperature sintering. J Clean Prod [Internet]. 2021;278:123985. Available from http://www.sciencedirect.com/science/article/pii/S0959652620340300.
8. Ross CP, Tincher GL, Rasmussen M. Glass melting technology: a technical and economic assessment. October; 2004. p. 1–292.
9. Ska B. FERVER Statistics for 2014-2018 [Internet]. Eurostat Recycling Rate Glass Packaging. 2018. Available from: https://www.ferver.eu/en/statistics
10. Schott O. Glass. United States. 1915;p. 1.
11. Wu PP, Zhang C, Xu HF, Huang DX, Xu B, Jiang DY. Corrosion behaviors of borosilicate glasses in various leaching agents. Adv Mater Res. 2010;177:466–9.
12. Lima MM, Monteiro R. Characterisation and thermal behaviour of a borosilicate glass. Thermochim Acta. 2001;373:69–74.
13. Zawrah MF, Hamzawy E. Effect of cristobalite formation on sinterability, microstructure and properties of glass/ceramic composites. Ceram Int. 2002;28:123–30.
14. Lee S, Park J. Mechanism of preventing crystallization in low-firing glass/ceramic composite substrates. J Am Ceram Soc. 1995;78(4):1128–32.
15. Rincon Romero A, Tamburini S, Taveri G. Extension of the ' inorganic gel casting ' process to the foams, boro-alumino-silicate Glass. Materials (Basel). 2018;11:2545–50.
16. Rincon Romero A, Salvo M, Bernardo E. Up-cycling of vitrified bottom ash from MSWI into glass-ceramic foams by means of 'inorganic gel casting' and sinter-crystallization. Constr Build Mater. 2018;192:133–40. Available from: https://doi.org/10.1016/j.conbuildmat.2018.10.135
17. Bai C, Li H, Bernardo E, Colombo P. Waste-to-resource preparation of glass-containing foams from geopolymers. Ceram Int. 2019;45(6):7196–202. Available from: https://doi.org/10.1016/j.ceramint.2018.12.227
18. Rincon Romero A, Toniolo N, Boccaccini AR. Glass-ceramic foams from 'weak alkali activation' and gel-casting of waste glass/fly ash mixtures. Materials. 2019;12(4):588.
19. Petersen RR, König J, Yue Y. The viscosity window of the silicate glass foam production. J Non Cryst Solids [Internet]. 2017;456:49–54. Available from https://www.sciencedirect.com/science/article/pii/S0022309316304835.
20. Provis JL. Geopolymers and other alkali activated materials: Why, how and what? 2014;11–25.
21. Taveri G, Tousek J, Bernardo E, Toniolo N, Boccaccini AR, Dlouhy I. Proving the role of boron in the structure of fly-ash / borosilicate glass based geopolymers. Mater Lett [Internet]. 2017;200:105–8. https://doi.org/10.1016/j.matlet.2017.04.107
22. He J, Zhang J, Yu Y, Zhang G. The strength and microstructure of two geopolymers derived from metakaolin and red mud-fly ash admixture : a comparative study. Constr Build Mater. 2012;30:80–91. https://doi.org/10.1016/j.conbuildmat.2011.12.011
23. Riahi S, Nazari A, Zaarei D, Khalaj G, Bohlooli H. Compressive strength of ash-based geopolymers at early ages designed by Taguchi method Compressive strength of ash-based geopolymers at early ages designed by Taguchi method. Mater Des [Internet]. 2012;37(May):443–9. https://doi.org/10.1016/j.matdes.2012.01.030
24. Blasenbauer D, Huber F, Lederer J, Quina MJ, Blanc-Biscarat D, Bogush A, et al. Legal situation and current practice of waste incineration bottom ash utilisation in Europe. Waste Manag. 2020;102:868–83.
25. Lee MY, Tan J, Heng JYY, Cheeseman C. A comparative study of production of glass microspheres by using thermal process. IOP Conf Ser Mater Sci Eng [Internet]. 2017;205:120–2.
26. Gibson I, Momeni A, Filiaggi M. Minocycline-loaded calcium polyphosphate glass microspheres as a potential drug-delivery agent for the treatment of periodontitis. J Appl Biomater Funct Mater. 2019;17(3):228080001986363. https://doi.org/10.1177/2280800019863637.
27. Wang L, Aslani F, Hajirasouliha I, Roquino E. Ultra-lightweight engineered cementitious composite using waste recycled hollow glass microspheres. J Cleaner Prod. 2020;249:119331.
28. MLaren JS, Macri-Pellizzeri L, Hossain KMZ, Patel U, Grant DM, Scammell BE, et al. Porous phosphate-based glass microspheres show biocompatibility, tissue in filtration, and osteogenic onset in an ovine bone defect model. Appl Mater Interfaces. 2019;11:15436–46.
29. Cheng Z, Wang F, Wang H, Liang H, Ma L. Effect of embedded polydisperse glass microspheres on radiative cooling of a coating. Int J Thermal Sci. 2019;140:358–67
30. Righini GC. Glassy microspheres for energy applications. Micromachines. 2018;9(8):379.
31. Kraxner J. Utility model of equipment for the production of solid and hollow glass and glass ceramic microspheres by flame synthesis. Slovakia; 8673, 2020.
32. Prnová A, Valúchová J, Parchoviansky M, Wisniewski W, Van PŠ, Klement R, et al. $Y_3Al_5O_{12}$-α-Al_2O_3 composites with fine-grained microstructure by hot pressing of Al_2O_3-Y_2O_3 glass microspheres. J Eur Ceram Soc. 2020;40(3):852–60.
33. Majerová M, Škrátek M, Prnová A, Dvurečenskij A, Kraxner J, Švančárek P, et al. Preparation and characterization of Ni doped

$Ca_2Al_2SiO_7$ glass microspheres. In: MEASUREMENT 2019, Proceedings of the 12th International ConferenceSmolenice, Slovakia. 2019. p. 282–5.
34. Shira S, Buller C. 11 - Mixing and Dispersion of Hollow Glass Microsphere Products. In: Amos SE, Yalcin Elastomers, and Adhesives Compounds BBT-HGM for P, editors. Plastics design library [Internet]. Oxford: William Andrew Publishing. 2015; p. 241–71. Available from: http://www.sciencedirect.com/science/article/pii/B9781455774432000116
35. Perfilov VA, Oreshkin DV, Semenov VS. Environmentally safe mortar and grouting solutions with hollow. Procedia Eng [Internet]. 2016;150:1479–84. Available from: https://doi.org/10.1016/j.proeng.2016.07.086
36. Oreshkin D, Semenov V, Rozovskaya T. Properties of light-weight extruded concrete with hollow glass microspheres. Procedia Eng. 2016;153:638–43. https://doi.org/10.1016/j.proeng.2016.08.214
37. Al-gemeel AN, Zhuge Y, Youssf O. Use of hollow glass microspheres and hybrid fibres to improve the mechanical properties of engineered cementitious composite. Constr Build Mater [Internet]. 2018;171:858–70. https://doi.org/10.1016/j.conbuildmat.2018.03.172
38. Schmid GHS, Bauer J, Eder A, Eisenmenger-sittner C. A hybrid hydrolytic hydrogen storage system based on catalyst-coated hollow glass microspheres. Int J Energy Res. 2017;41(2):297–314.
39. Zhao K, Liu H, Wang T, Zeng H. Cu-plated hollow glass microspheres for hydrogen production and degradation. J Mater Sci Mater Electron. 2016;27(5):5183–9.
40. Dalai S, Vijayalakshmi S, Shrivastava P, Param S, Sharma P. Preparation and characterization of hollow glass microspheres (HGMs) for hydrogen storage using urea as a blowing agent. Microelectr Eng. 2014;126:65–70.
41. Dalai S, Vijayalakshmi S, Sharma P, Yeon K. Magnesium and iron loaded hollow glass microspheres (HGMs) for hydrogen storage. Int J Hydrogen Energy [Internet]. 2014;39(29):16451–8.
42. Wang X, Zhao H, Li A, Tian K, Brambilla G, Wang P. Near-infrared luminescence and single-mode laser emission from Nd^{3+}. Doped Compound Glass Glass Microsphere. 2019;6(September):1–6.
43. Soler-carracedo K, Ruiz A, Martín IR, Lahoz F. Luminescence whispering gallery modes in Ho 3 þ doped microresonator glasses for temperature sensing. J Alloys Compd [Internet]. 2019;777:198–203.
44. Li A, Dong Y, Wang S, Jia S, Brambilla G, Wang P. Infrared-laser and upconversion luminescence in Ho 3 þ -Yb 3 þ codoped tellurite glass microsphere. J Lumin [Internet]. 2020;218(September 2019):116826.
45. Pontiroli L, Dadkhah M, Novajra G, Tcacencu I, Fiorilli S, Vitale-brovarone C. An aerosol-spray-assisted approach to produce mesoporous bioactive glass microspheres under mild acidic aqueous conditions. Mater Lett. 2017;190:111–4. https://doi.org/10.1016/j.matlet.2016.12.125
46. Kraxner J, Michalek M, Rincon A, Elsayed H, Bernardo E, Boccaccini AR, et al. Porous bioactive glass microspheres prepared by flame synthesis process. Mater Lett. 2019;256:126625.
47. Todea M, Turcu RVF, Frentiu B, Simon S. FTIR and NMR evidence of aluminosilicate microspheres bioactivity tested in simulated body fluid. J Non-Crystalline Solids. 2016;432:413–9.
48. Optimizing metal powders for additive manufacturing [Internet]. Limited, Malvern Instruments. 2017. Available from https://www.additivemanufacturing.media/articles/optimizing-metal-powders-for-additive-manufacturing-exploring-the-impact-of-particle-morphology-and-powder-flowability.
49. Akowanou AVO, Deguenon HEJ, Groendijk L, Aina MP, Yao BK, Drogui P. 3D-printed clay-based ceramic water filters for point-of-use water treatment applications. Prog Addit Manuf [Internet]. 2019;4(3):315–21.
50. Ashby MF. Materials and environment. Oxford, UK: Buttersworth-Heinemann; 2013. p. 628.
51. Rincon Romero A, Elsayed H, Bernardo E. Highly porous mullite ceramics from engineered alkali activated suspensions. J Am Ceram Soc. 2017;101:1036–41.
52. Farcomeni A, Serranti S, Bonifazi G. Non-parametric analysis of infrared spectra for recognition of glass and glass ceramic fragments in recycling plants. Waste Manag. 2008;28(3):557–64.
53. Semnani D. Geometrical characterization of electrospun nanofibers. Electrospun Nanofibers. 2017;p. 151–80.
54. Datsiou KC, Saleh E, Spirrett F, Goodridge R, Ashcroft I, Eustice D. Additive manufacturing of glass with laser powder bed fusion. J Am Ceram Soc. 2019;102(8):4410–4.
55. Hench LL, Clark DE. Physical chemistry of glass surfaces. J Non Cryst Solids. 1978;28:83–105.
56. Rincon Romero A, Desideri D, Bernardo E. Functional glass-ceramic foams from 'inorganic gel casting' and sintering of glass/slag mixtures. J Clean Prod. 2018;187:250–6.

How to cite this article: Larionau P, Hujova M, Michalková M, Mahmoud M, Švančárková A, Galusková D, et al. Low-alkali borosilicate glass microspheres from waste cullet prepared by flame synthesis. *Int J Appl Glass Sci*. 2021;12:562–569. https://doi.org/10.1111/ijag.16144